Kovove Mater. 52 2014 305–311
DOI: 10.4149/km_2014_5_305

Microstructure characteristics of Ti-2Al-Mn/Al1060 dissimilar joint by pulsed gas metal arc welding-brazing

S. Wei, Y. Li*, J. Wang, K. Liu, P. Zhang

Key Laboratory for Liquid-Solid Structural Evolution and Processing of Materials (Ministry of Education), Shandong University, Jinan 250061, P. R. China

Received 27 March 2013, received in revised form 17 April 2014, accepted 17 April 2014

Abstract

Butt welding-brazing of titanium alloy Ti-2Al-Mn to aluminum 1060 plates was investigated by pulsed gas metal arc welding using an AlSi5 filler wire. Microstructure characteristics of Ti/Al dissimilar joint were observed by scanning electron microscope. Chemical composition and phase constituent of Ti-Al transition region were investigated using energy-dispersive spectrometer and X-ray diffraction. Micro-hardness distribution of the weld zone was tested by micro-sclerometer. The experiment results indicated that joint free of pores and cracks could be obtained by controlling the welding process. The weld metal was composed of α-Al dendrites and α-Al+Si eutectic phase. The intermetallic compound $TiAl_3$ appeared in the weld metal. A multilayered Ti-Al transition region containing $TiAl_3$, $Ti_7Al_5Si_{12}$ and α-Ti had formed adjacent to the Ti/Al interface. Micro-hardness of the transition region was about 280 $HV_{0.05}$. The heat-affected zone of Ti-2Al-Mn alloy was mainly composed of acicular α' and lath α' martensite phases. Micro-hardness of the heat-affected zone was 220–270 $HV_{0.05}$.

K e y w o r d s: Ti-2Al-Mn alloy, Al1060, pulsed gas metal arc welding, microstructure, micro-hardness

1. Introduction

Due to the demand for light-weight constructions to reduce fuel consumption, titanium and aluminum alloys are widely used in aerospace and automobile industries. Ti/Al hybrid structures have advantages in comparison to single material [1]. However, a key issue encountered in welding titanium alloy to aluminum alloy is the formation of brittle intermetallic compounds, which would seriously degrade the mechanical properties of the Ti/Al dissimilar joint. In order to suppress the growth of brittle intermetallic compounds, attempts were conducted by laser welding--brazing [1–3], gas tungsten arc welding-brazing [4], friction stir welding [5–7], diffusion bonding [8–10] and brazing [11, 12].

The feasibility of laser welding-brazing in joining titanium alloy to aluminum alloy was demonstrated by M. Kremeyer et al. By melting titanium alloy, Ti--6Al-4V and AA6016 alloys were successfully joined together [1]. But other researchers had found that Ti/Al welded-brazed joint had much higher properties by melting aluminum alloy [2, 13–15]. Butt joining of titanium alloy to aluminum alloy by gas tungsten arc welding-brazing using an AlSi12 eutectic filler wire without flux was investigated by Z. Ma et al. [4]. However, laser processing may be unsuitable for practical mass manufacturing because of the high costs of the equipments. Compared with laser processing, gas metal arc welding (GMAW) costs less and has a much broader applicability. Pulsed gas metal arc welding (P-GMAW) has the characteristic in controlling welding heat-input accurately. And weld depth-to--width ratio is higher than that of traditional GMAW process. In the present study, pulsed gas metal arc welding-brazing of titanium alloy Ti-2Al-Mn to aluminum 1060 was investigated using AlSi5 filler metal. The objective of the research was to study the microstructure characteristics of the welded-brazed joint. It also aimed to determine the chemical composition and the phase constituent of the Ti-Al transition region.

*Corresponding author: tel.: +86 531 88392924; e-mail address: yajli@sdu.edu.cn

Table 1. Chemical composition and physical properties of experimental materials

Experimental materials	Chemical composition (wt.%)							Physical properties			
	Al	Ti	Mn	Fe	Si	Mg	Cu	Density ($g\,cm^{-1}$)	Melting temperature (℃)	Thermal conductivity ($W\,m^{-1}\,K^{-1}$)	Coefficient of linear expansion ($10^{-6}\,K^{-1}$)
Al 1060	Bal.	0.03	0.03	0.25	0.05	0.03	–	2.7	657	243	23.6
Ti-2Al-Mn alloy	1.8	Bal.	1.0	0.3	–	–	–	4.6	1630	10.2	8.0
AlSi5 wire	Bal.	0.20	0.05	0.80	5.3	0.0.5	0.30				

Table 2. Parameters of pulsed gas metal arc welding-brazing

Parameters	Filler metal (cm)	Arc voltage (V)	Current level (A)	Welding speed ($cm\,s^{-1}$)	Wire feed rate ($m\,min^{-1}$)	Heat input ($kJ\,cm^{-1}$)	Argon flow rate ($l\,min^{-1}$)
Value	AlSi5 (φ 1.2)	14.2–15.2	40–46	0.33	2.2	1.71–2.10	14–16

2. Experimental methods

Compared with other titanium alloys, Ti-2Al-Mn alloy has relatively good weldability, so titanium alloy Ti-2Al-Mn and aluminum 1060 plates with dimensions of 200 mm × 50 mm × 1.5 mm were used as the experimental materials. Elemental Si had been demonstrated to be highly effective in suppressing the growth rate of Ti-Al intermetallic compounds [16], so the near eutectic AlSi5 wire with diameter of 1.2 mm was used as filler metal. Microstructure of Ti-2Al-Mn and Al1060 parent metal is shown in Fig. 1. Equiaxed α and intergranular β phases coexisted in Ti-2Al-Mn alloy. Al1060 is composed of α-Al solid solutions. Nominal chemical composition and physical properties of the experimental materials are listed in Table 1. Both Ti-2Al-Mn alloy and Al1060 are active light metals, and parent metals need strictly cleaning up before welding. Oxidation films were removed by grinding process. The surfaces of samples were cleaned by alkali liquor (NaOH 8 vol.%, H_2O 92 vol.%). At last, all the plates were cleaned in alcoholic solution and dried.

The titanium alloy Ti-2Al-Mn and Al1060 were arranged in butt joint without groove. The welding--brazing process was carried out using Fronius TPS--4000 CMT welding equipment at room temperature. The AlSi5 filler wire was fed automatically using Fronius VR 4000 wire feeding device. The wire extension was 12 mm. Argon shield gas was used to protect both sides of the liquid mixed metal from oxidation. The argon flow rate was 14–16 $l\,min^{-1}$. The welding heat input was controlled in the range of 1.71–2.10 $kJ\,cm^{-1}$. Parameters of pulsed gas metal arc welding--brazing are listed in Table 2.

After welding, the joints cross-sections perpendicular to the welding direction were grinded and polished. All the samples were etched by chemical etchants (20 vol.% HF, 20 vol.% HNO_3 and 60 vol.% H_2O) for 5–10 s. Microstructure characteristics and chem-

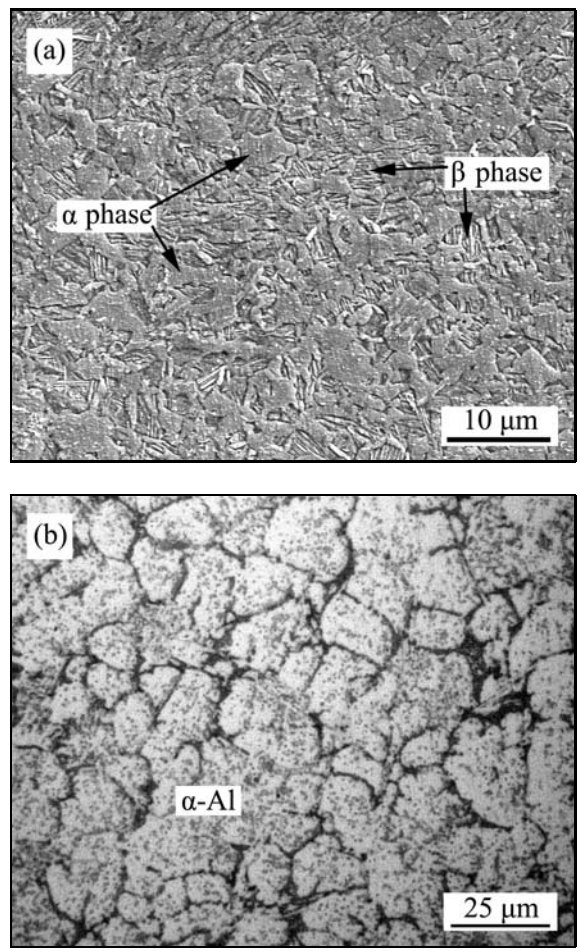

Fig. 1. Microstructure of Ti-2Al-Mn parent metal: titanium alloy Ti-2Al-Mn (a), aluminum 1060 (b).

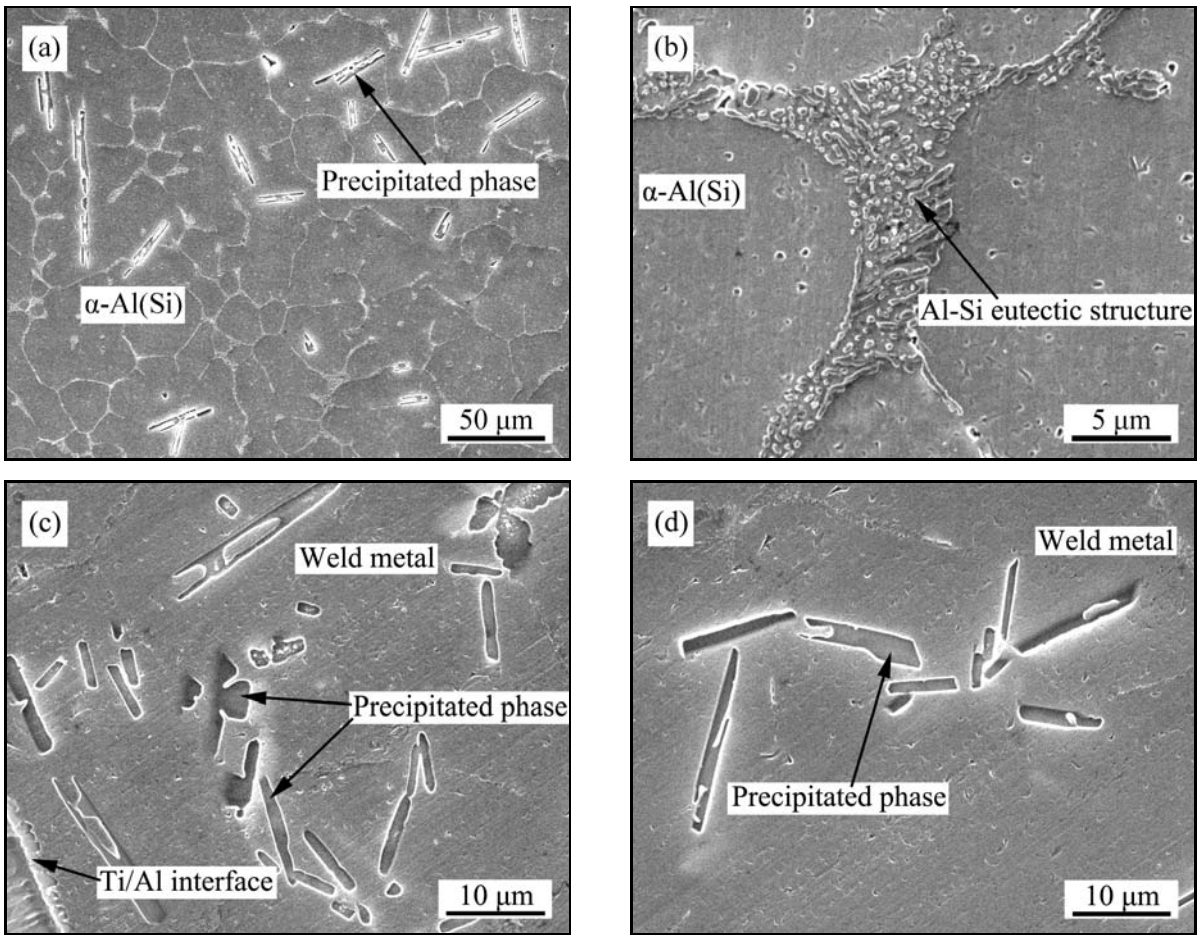

Fig. 2. Microstructure of the weld metal: α-Al dendrites (a), α-Al + Si eutectic structures (b), precipitation near the Ti/Al interface (c), precipitation away from the Ti/Al interface (d).

ical composition of the welded-brazed joint were examined using HITACHI SU-70 scanning electron microscope (SEM) equipped with an energy-dispersive spectrometer (EDS). The phase constitution of the Ti-Al transition region was identified by D/MAX-RC X-ray diffraction (XRD). Micro-hardness distribution of the weld zone was measured at intervals of 0.10 mm by DHV-1000 micro-sclerometer with a load of 0.05 kg for 10 s.

3. Results and discussion

3.1. Microstructure of the weld metal

Owing to influence of heat source, Al1060 and AlSi5 filler metal were melted and mixed integrated. Consequently, a fusion zone with hypoeutectic microstructure was formed at the Al1060 side. At the same time, Ti-2Al-Mn alloy in solid state interacted with liquid mixed metal, and a complex Ti-Al transition region was formed at the Ti-2Al-Mn side. No voids and cracks were observed in the joint indicating good combination of Ti-2Al-Mn alloy with Al1060.

Microstructure of the weld metal is shown in Fig. 2a. Chemical composition of weld metal was analyzed using energy-dispersive spectrometer (EDS). The results showed that the weld metal was composed of α-Al dendrites and α-Al + Si eutectic phase. During the cooling process after welding, solidification and crystallization of the molten metal was rapid. According to Al-Si binary phase diagram [17], α-Al grains with a small dissolution of Si started to crystallize firstly. Concentration of Si in the liquid metal ascended with the dropping of temperature. Owing to constituent fluctuations and temperature fluctuations, α-Al grains grew into coarse dendrites. In the end, concentration of Si in liquid metal approached the Al-Si eutectic point. Thus α-Al + Si eutectic structures were formed along the boundaries of α-Al grains, as shown in Fig. 2b.

As shown in Fig. 2c,d, a few blocky and rod-like precipitations appeared in the weld metal. And the precipitations were mostly distributed near the Ti/Al interface. Chemical composition of the precipitation was analyzed using EDS. Atomic percentage of Ti in

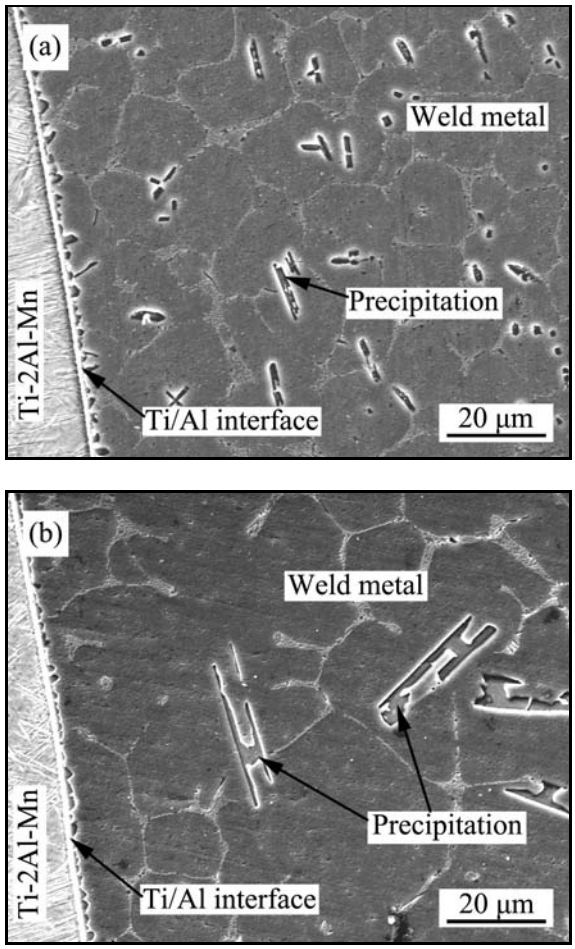

Fig. 3. Precipitation in weld metal with different welding heat input: 1.80 kJ cm^{-1} (a), 2.00 kJ cm^{-1} (b).

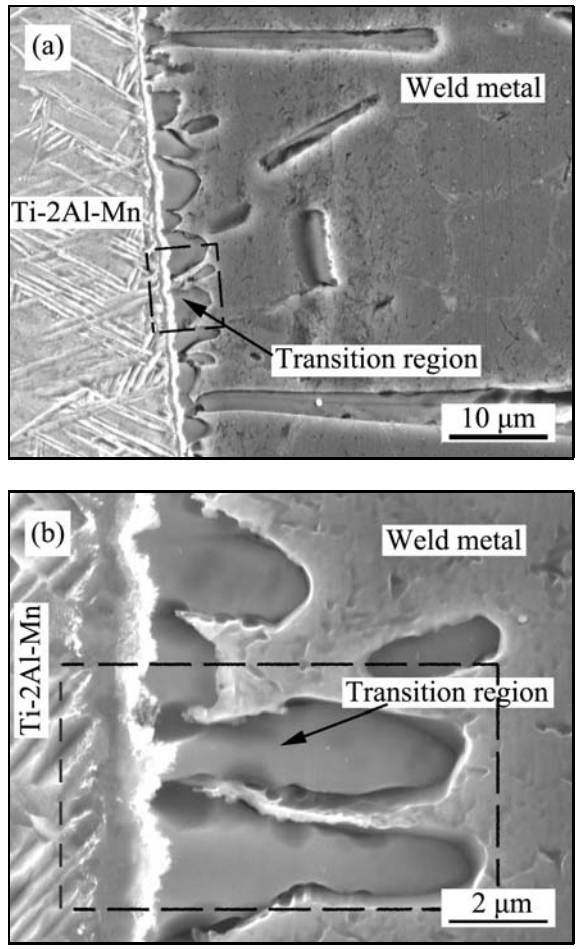

Fig. 4. Microstructure of Ti-Al transition region: with a low magnification (a), with a high magnification (b).

the precipitation was 25 at.%, Al was 71 at.%, Si was 4 at.%. Atomic ratio of Ti to Al was approximately equal to 1 : 3. It is obvious that the precipitation is mainly composed of binary intermetallic compound $TiAl_3$. During the welding-brazing process, Ti atoms gradually diffused from the solid-liquid interface to the molten metal as the Ti-2Al-Mn alloy parent metal was continuously dissolved into the liquid metal. Concentration of Ti in the molten metal gradually ascended to a high level, and intermetallic $TiAl_3$ was generated firstly in the liquid metal. Potential energy of Si in solid $TiAl_3$ was much lower than that in liquid metal. A few Si atoms substituted for Al in the ordered lattice of $TiAl_3$ at elevated temperature [15]. Thus the precipitation was actually composed of $TiAl_3$ with a small dissolution of Si. The research found that $TiAl_3$ precipitation could form into tiny particles by controlling the welding heat input, as shown in Fig. 3. The tiny $TiAl_3$ precipitations created heterogeneous nucleation condition for molten pool. And liquid metal crystallized into relatively fine α-Al grains. The refinement of precipitation on weld metal improved the toughness of weld metal.

3.2. Microstructure of the Ti-Al transition region

According to Ti-Al binary phase diagram, reactions of Ti and Al take place at elevated temperature over 665 ℃. During the welding-brazing process, owing to interactions of solid Ti-2Al-Mn and liquid metal, Ti-Al intermetallic compounds such as $TiAl_3$ were generated adjacent to the Ti/Al interface. The intermetallics had definite brittleness and were unfavorable to the combination of Ti-2Al-Mn and Al1060. But a previous study stated that the intermetallics did little harm to the properties of Ti/Al joint if the width of the intermetallics layer was less than 10 μm [1].

Microstructures of the Ti-Al transition region with different magnifications are shown in Fig. 4a,b. A complex Ti-Al transition region had formed adjacent to the Ti/Al interface. And the average width of the transition region was less than 10 μm. Neither pores nor cracks had been obviously observed in the region near the Ti/Al interface. According to Fig. 4b, a serrate layer, a bright thin layer and a gray thin

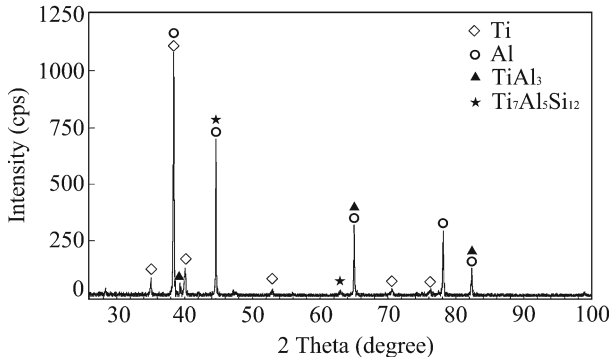

Fig. 5. XRD pattern of the Ti-Al transition region.

Table 3. Chemical composition at locations A–E (at.%)

Locations	Ti	Al	Si	Mn
A	96.67	2.18	0	1.15
B	85.31	12.16	2.09	0.44
C	29.19	58.70	12.11	0
D	23.85	71.52	4.63	0
E	3.19	94.38	2.43	0

layer were formed orderly from the weld metal to titanium alloy Ti-2Al-Mn. The peak temperature in liquid mixed metal was high in the welding-brazing process. Reactions of Ti and Al were rapid and sufficient, and Ti-Al intermetallics were generated at the Ti/Al interface. Because crystallization conditions of different intermetallics are different, Ti-Al intermetallics crystallized adjacent to the Ti/Al interface in a sorted order. Eventually a multilayered transition region was formed. Phase constituent of Ti-Al transition region was examined by XRD, and the pattern is given in Fig. 5. According to the observation, binary intermetallic compound $TiAl_3$ and ternary intermetallic compound $Ti_7Al_5Si_{12}$ were formed adjacent to the Ti/Al interface.

In order to analyze the detailed chemical composition of Ti-Al transition region with a welding heat input of 2.10 kJ cm^{-1}, selected locations marked as A, B, C, D and E in Fig. 6a were analyzed using EDS and the results are listed in Table 3. To further identify the phase distribution, line scanning analysis across the transition region was carried out using EDS, and the result is shown in Fig. 6b. According to EDS results, atomic ratio of Ti to Al was approximately equal to 1: 3 in the serrate layer, so the serrate layer was mainly composed of $TiAl_3$ with 5 at.% dissolved Si. The atomic percent of Si in the bright reaction layer was much higher than that in other layers. According to phase constituent analysis by XRD, the bright thin layer is mostly composed of ternary intermetallic

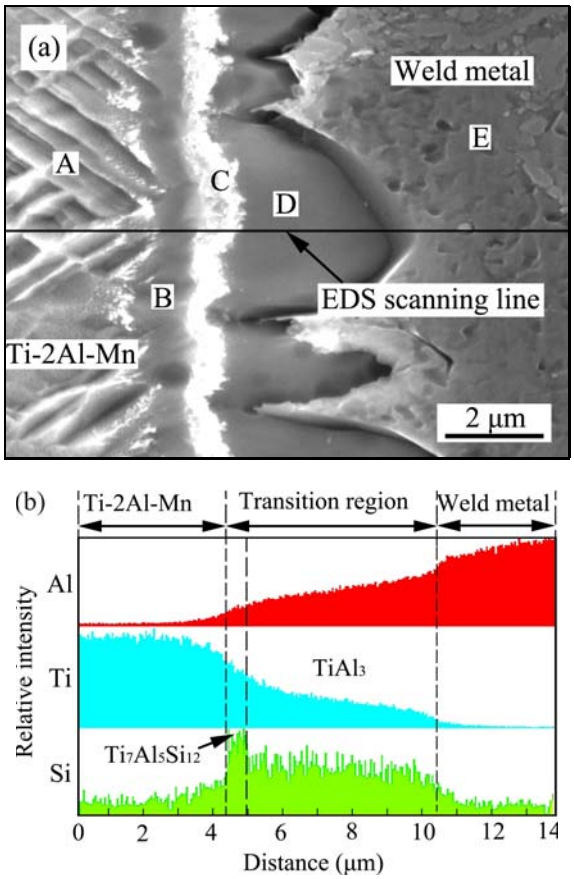

Fig. 6. EDS analysis of the Ti-Al transition region: test locations of EDS analysis (a), results of EDS line scanning analysis (b).

compound $Ti_7Al_5Si_{12}$. Atomic percents of Al and Si in the gray reaction layer were determined to be 12 % and 2 %, respectively. During the welding-brazing process, a number of Al and Si atoms diffused across the Ti/Al interface into the Ti-2Al-Mn parent metal. Phase transformation from α to β was suppressed by the presence of Al. Thus the gray layer was composed of α-Ti solid solution.

3.3. Microstructure of heat-affected zone in Ti-2Al-Mn alloy

Owing to heat conduction from the liquid metal, temperature of Ti-2Al-Mn parent metal near the molten pool ascended to an elevated temperature upper than $\beta \rightarrow \alpha$ transformation temperature. During the cooling process, transformation of β phase to α phase could not be achieved when the titanium alloy was cooled down at a high cooling rate. Then β phase would transform into a kind of supersaturated solid solution, called the martensite phase. Because the element Mn could strongly lower the $\beta \rightarrow \alpha$ transformation temperature, β phase mainly transformed into the

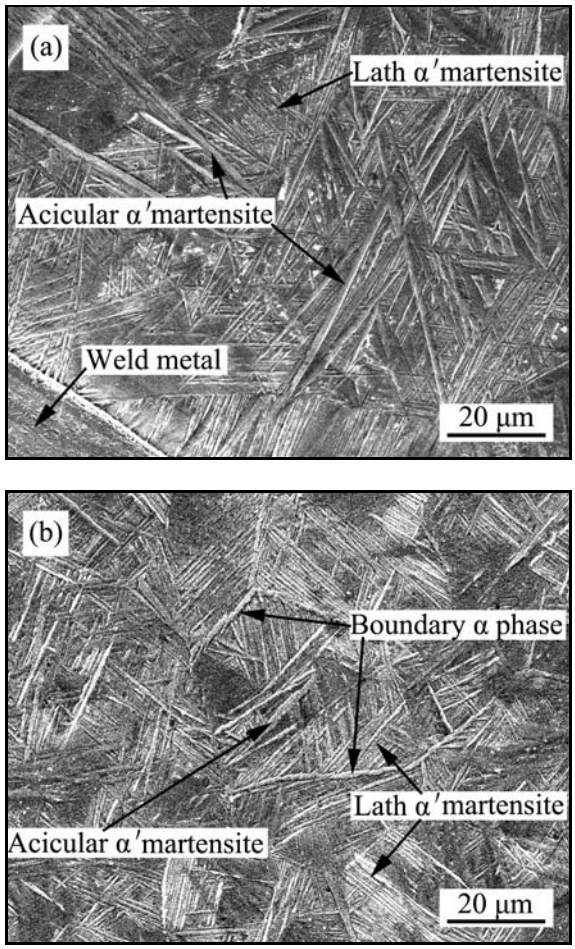

Fig. 7. Microstructure of heat-affected zone of Ti-2Al-Mn alloy: (a) coarse grain region, (b) fine grain region.

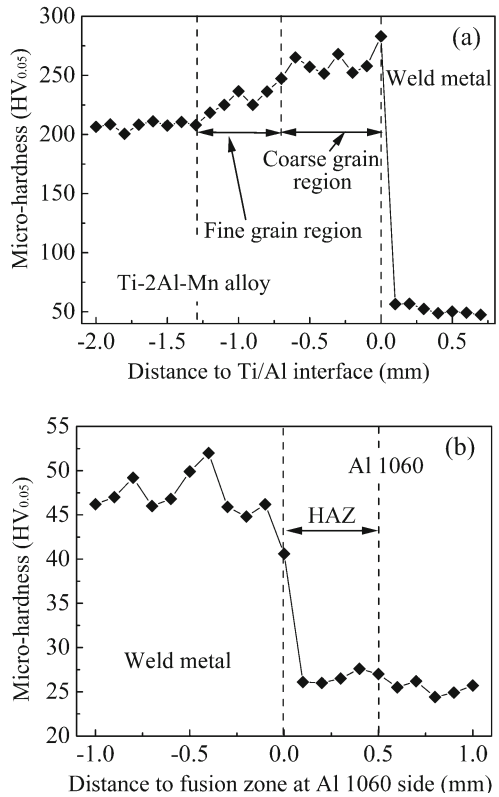

Fig. 8. Micro-hardness distribution of the joint: near the Ti/Al interface (a), near the fusion zone at Al1060 side (b).

α' martensite with the hexagonal close-packed (HCP) structure.

Microstructure of heat-affected zone (HAZ) in Ti-2Al-Mn alloy is shown in Fig. 7. There were two kinds of α' martensite phases in the HAZ. According to the observation, the HAZ could be divided into coarse grain region and fine grain region. The coarse grain region was adjacent to the weld metal. Microstructure of coarse grain region is shown in Fig. 7a. During the cooling process following welding, cooling rate of the coarse grain region was high. And β phase mainly transformed into the acicular α' martensite as $\beta \rightarrow \alpha$ transformation temperature was low. Thus the coarse grain region was mainly composed of acicular α' martensite. A few lath α' martensite existed in the coarse grain region, too.

Microstructure of fine grain region of heat-affected zone is shown in Fig. 7b. During the welding-brazing process, the peak temperature that fine grain region endured was just a little higher than $\beta \rightarrow \alpha$ phase transformation temperature [18]. Because of thermal conduction from molten pool, the cooling rate of fine grain region was not as high as coarse grain region. These factors resulted in reduction of acicular α' martensite phase. Thus fine grain region was mainly composed of lath α' martensite but a few acicular α' phases. The boundary α phase was vaguely visible in this region. No α'' martensite was observed in the HAZ indicating good properties of the parent metal.

3.4. Micro-hardness distribution of the Ti/Al joint

During the welding-brazing process, intermetallic $TiAl_3$ was generated in the weld metal, a complex transition region was formed adjacent to the Ti/Al interface, and phase transformation occurred in the HAZ of Ti-2Al-Mn alloy. All of these factors resulted in change of micro-hardness distribution in the joint. Micro-hardness distribution near the Ti/Al interface is shown in Fig. 8a. The Ti-Al transition region was mainly composed of intermetallic $TiAl_3$. Width of $TiAl_3$ layer was so thin that micro-hardness value of the transition region was influenced by materials on both sides. Thus micro-hardness of the transition region was about 280 $HV_{0.05}$, which was lower than that reported by other researchers [11]. There were lath α' and acicular α' martensite in the heat-affected zone of

Ti-2Al-Mn. Because hardness of acicular α' phase was higher than lath α' phase, micro-hardness of the coarse grain region was 240–270 $HV_{0.05}$, and micro-hardness of the fine grain region was a little lower, which was 220–240 $HV_{0.05}$. Micro-hardness of Ti-2Al-Mn parent metal was 200–210 $HV_{0.05}$.

Micro-hardness distribution near fusion zone at Al1060 side is shown in Fig. 8b. No defects such as voids or pores were found near the fusion zone. The weld metal was composed of α-Al dendrites and α-Al + Si eutectic phase, and micro-hardness of the weld metal was 40–50 $HV_{0.05}$. The fusion zone was formed by the mixture of partly melted Al1060 with the AlSi5 liquid metal. And the micro-hardness of the fusion zone was a little lower than that of weld metal but higher than that of Al1060 (35–40 $HV_{0.05}$). Micro-hardness in the HAZ of Al1060 was close to the parent metal, approximately 25–30 $HV_{0.05}$.

4. Conclusions

1. Titanium alloy Ti-2Al-Mn and aluminum 1060 were successfully joined together by pulsed gas metal arc welding-brazing using AlSi5 filler metal. Joint free of pores and cracks could be achieved by controlling the welding process.

2. The weld metal was composed of α-Al dendrites and α-Al + Si eutectic phase. Blocky and rod-like $TiAl_3$ precipitation appeared in the weld metal. A multilayered Ti-Al transition region containing serrate $TiAl_3$ layer, bright $Ti_7Al_5Si_{12}$ layer and gray α-Ti layer had formed adjacent to the Ti/Al interface. Heat-affected zone (HAZ) of Ti-2Al-Mn alloy was mainly composed of acicular α' and lath α' martensite phases.

3. Micro-hardness of the weld metal was 45–50 $HV_{0.05}$. Micro-hardness of the Ti-Al transition region was 270–280 $HV_{0.05}$. Micro-hardness of coarse grain region and fine grain region of Ti-2Al-Mn alloy were 220–240 $HV_{0.05}$ and 240–270 $HV_{0.05}$, respectively.

Acknowledgement

This research was supported by the National Natural Science Foundation of China (No. 51175303). The authors express heartfelt thanks here.

References

[1] Kreimeyer, M., Wagner, F., Vollertsen, F.: Opt Lasers Eng., *43*, 2005, p. 1021. doi:10.1016/j.optlaseng.2004.07.005
[2] Möller, F., Garden, M., Thomas, C., Vollertsen, F.: Physics Procedia., *12*, 2011, p. 215. doi:10.1016/j.phpro.2011.03.028
[3] Chen, Y. B., Chen, S. H., Li, L. Q.: Int J Adv Manuf Technol., *44*, 2009, p. 265. doi:10.1007/s00170-008-1837-2
[4] Ma, Z. P., Wang, C. W., Yu, H. C., Yan, J. C., Shen, H. R.: Mater Des, *45*, 2013, p. 72. doi:10.1016/j.matdes.2012.09.007
[5] Dressler, U., Biallas, G., Alfaro Mercado, U.: Mater Sci Eng A., *526*, 2009, p. 113. doi:10.1016/j.msea.2009.07.006
[6] Chen, Y. C., Nakata, K.: Mater Des., *30*, 2009, p. 469. doi:10.1016/j.matdes.2008.06.008
[7] Wei, Y. N., Li, J. L., Xiong, J. T., Huang, F., Zhang, F. S., Raza, S. H.: Mater Charact., *71*, 2012, p. 1. doi:10.1016/j.matchar.2012.05.013
[8] Ustinov, A. I., Falchenko, Yu. V., Ishchenko, A. Ya., Kharchenko, G. K., Melnichenko, T. V., Muraveynik, A. N.: Intermetallics, *16*, 2008, p. 1043. doi:10.1016/j.intermet.2008.05.002
[9] Kenevisi, M. S., Mousavi Khoie, S. M.: Mater Lett., *76*, 2012, p. 144. doi:10.1016/j.matlet.2012.02.104
[10] Alhazaa, A. N., Khan, T. I.: J Alloy Compd., *494*, 2010, p. 351. doi:10.1016/j.jallcom.2010.01.037
[11] Song, Z., Nakata, K., Wu, A. P., Liao, J. S.: Mater Sci Eng A., *560*, 2013, p. 111. doi:10.1016/j.msea.2012.09.044
[12] Zhu, Z. Q., Lee, K. Y., Wang, X. L.: Int J Adv Manuf Technol., *59*, 2012, p. 569. doi:10.1007/s00170-011-3534-9
[13] Chen, S. H., Li, L. Q., Chen, Y. B., Huang, J. H.: J Alloy Compd., *509*, 2011, p. 891. doi:10.1016/j.jallcom.2010.09.125
[14] Chen, Y. B., Chen, S. H., Li, L. Q.: Mater Des., *31*, 2010, p. 227. doi:10.1016/j.matdes.2009.06.029
[15] Chen, S. H., Li, L. Q., Chen, Y. B., Liu, D. J.: Trans Nonferr Met Soc China, *20*, 2010, p. 64. doi:10.1016/S1003-6326(09)60098-4
[16] Enjo, T., Ikeuchi, K., Horinouchi, T.: Trans JWRI, *15*, 1986, p. 61.
[17] Zhang, Q. Y., Zhuang, H. S.: Brazing and Soldering Manual. Beijing, China Machine Press 2008.
[18] Yang, J., Cheng, D. H., Huang, J. H., Zhang, H., Zhao, X. K., Guo, H. P.: Rare Metal Mat Eng., *38*, 2009, p. 259.